Spatially resolved assessment of hepatic function using 99mTc-IDA SPECT

Hesheng Wang[a)]
Department of Radiation Oncology, University of Michigan, 1500 East Medical Center Drive, Ann Arbor, Michigan 48109

Yue Cao
Department of Radiation Oncology, Radiology, and Biomedical Engineering, University of Michigan, 1500 East Medical Center Drive, Ann Arbor, Michigan 48109

(Received 25 January 2013; revised 24 June 2013; accepted for publication 11 July 2013; published 5 August 2013)

Purpose: 99mTc-iminodiacetic acid (IDA) hepatobiliary imaging is usually quantified for hepatic function on the entire liver or regions of interest (ROIs) in the liver. The authors presented a method to estimate the hepatic extraction fraction (HEF) voxel-by-voxel from single-photon emission computed tomography (SPECT)/CT with a 99mTc-labeled IDA agent of mebrofenin and evaluated the spatially resolved HEF measurements with an independent physiological measurement.
Methods: Fourteen patients with intrahepatic cancers were treated with radiation therapy (RT) and imaged by 99mTc-mebrofenin SPECT before and 1 month after RT. The dynamic SPECT volumes were with a resolution of $3.9 \times 3.9 \times 2.5$ mm^3. Throughout the whole liver with approximate 50 000 voxels, voxelwise HEF quantifications were estimated and compared between using arterial input function (AIF) from the heart and using vascular input function (VIF) from the spleen. The correlation between mean of the HEFs over the nontumor liver tissue and the overall liver function measured by Indocyanine green clearance half-time (T1/2) was assessed. Variation of the voxelwise estimation was evaluated in ROIs drawn in relatively homogeneous regions of the livers. The authors also examined effects of the time range parameter on the voxelwise HEF quantification.
Results: Mean of the HEFs over the liver estimated using AIF significantly correlated with the physiological measurement T1/2 ($r = 0.52$, $p = 0.0004$), and the correlation was greatly improved by using VIF ($r = 0.79$, $p < 0.0001$). The parameter of time range for the retention phase did not lead to a significant difference in the means of the HEFs in the ROIs. Using VIF and a retention phase time range of 7–30 min, the relative variation of the voxelwise HEF in the ROIs was 10% ± 6% of respective mean HEF.
Conclusions: The voxelwise HEF derived from 99mTc-IDA SPECT by the deconvolution analysis is feasible to assess the spatial distribution of hepatic function in the liver. [http://dx.doi.org/10.1118/1.4816655]

Key words: 99mTc-IDA SPECT, hepatic extraction fraction, hepatocyte function, liver dysfunction

1. INTRODUCTION

Scintigraphy and single-photon emission computed tomography (SPECT) with a 99mTc-labeled analog of iminodiacetic acid (IDA) is currently the only imaging-based hepatocellular function test in clinical settings. The clinical value of 99mTc-IDA SPECT has been demonstrated in diagnosis of various hepatobiliary diseases including acute hepatitis,[1] primary biliary cirrhosis,[2] acute jaundice,[3] and others.[4–6] Recently, SPECT with a 99mTc-labeled IDA derivative of mebrofenin has shown potential to assess liver function change in response to radiation therapy (RT).[7]

Following an intravenous injection, 99mTc-IDA is loosely bound to plasma proteins and carried to the liver. The IDA is extracted by the hepatocyte through an organic amino path, then transported across the hepatocytes into the bile canaliculi, and finally excreted through the bile ducts. Both scintigraphy and SPECT visualize the dynamic time course and thus provide information regarding hepatic extraction and secretion function.[8] From the dynamic time–activity curve, hepatic extraction fraction (HEF) of 99mTc-IDA is estimated to measure hepatic extraction function of the liver.[3,9] Using the IDA agent of 99mTc-mebrofenin, HEF is close to 1 in normal subjects and patients with near normal liver functions.[10] The decreases of HEF and the degree of HEF reduction are directly proportionate to the severity of hepatocyte dysfunction on patients with hepatocyte diseases.[9] However, due to low spatial resolution and limited detail of the images, HEF is usually quantified for the entire liver or regions of interest (ROIs) in the liver.[9–11] The lack of spatial discrimination in the HEF hampers a wider range use of IDA imaging in clinic, for examples, to assess regional hepatocyte dysfunction in the course of a treatment.

Today's technical advancements in hardware and software of SPECT enable us to acquire a dynamic, volumetric hepatobiliary SPECT with a spatial resolution of 3–4 mm,[12] which is significantly superior to the planar scintigraphy obtained 20 years ago. Moreover, the hybrid SPECT/CT system allows acquisition of functional and anatomical images within a single imaging session, and CT-based attenuation-correction

for SPECT.[13] In this study, using a hybrid SPECT/CT scanner, we aim to evaluate the feasibility of quantifying HEF on nontumor liver voxels from SPECT/CT with 99mTc-mebrofenin, which may enable spatial assessment of hepatic function.

To estimate the HEF from 99mTc-IDA images, a blood input function should be determined. The heart, the most common region to determine blood input function for ROI-based HEF quantification, may show large pulsation artifacts which may compromise the reproducibility of voxelwise quantification. With SPECT/CT, we were able to obtain blood input function from a ROI delineated on the spleen. We therefore compared the voxelwise HEF estimation from SPECT images using arterial input function (AIF) from the heart with that using vascular input function (VIF) from the spleen. To evaluate the spatially resolved HEF, we assessed the correlation between mean of estimated HEFs in the liver and an independent physiological measurement, i.e., Indocyanine green (ICG) clearance rate. Blood clearance of ICG is an objective test of overall liver function, and has been routinely used for planning of hepatectomy and liver transplantation.[14–16] Therefore, this study will evaluate the potential of 99mTc-IDA SPECT/CT to provide spatial assessment of hepatic function.

2. MATERIALS AND METHODS

2.A. SPECT/CT

Fourteen patients (1 woman and 13 men, 44–83 years old) with unresectable intrahepatic cancers participated in an institutional review board (IRB)-approved liver imaging study. Nine patients had hepatocellular carcinoma (HCC), three had cholangiocarcinoma, and the other two had metastases to the liver. The patients were treated with 3D conformal RT ($n = 3$, dose range: 50–64.8 Gy), intensity-modulated RT ($n = 3$, dose range: 50–54 Gy), or stereotactic body RT ($n = 8$, dose range: 17–50 Gy).

Dynamic SPECT of a patient was performed one week prior to RT and one month after the completion of RT. A Siemens hybrid SPECT/CT scanner (Symbia T6, Simens Medical Solutions) was used. After 3–4 h fast, the patient received an intravenous injection of 10 mCi 99mTc-mebrofenin. Dynamic data acquisition started immediately after the administration and lasted up to 60 min. The emission data were acquired by using parallel-hole, high-resolution collimators centered on the 140-keV photopeak with a 20% symmetrical window. The acquisition was in 64 projections (20 s per stop) with a noncircular orbit over 360° using a 128 × 128 matrix. A CT volume (matrix: 512 × 512 × 134; resolution: 1 × 1 × 2.5 mm^3) was acquired immediately after the dynamic SPECT with acquisition parameters of 130 kVp, 80 mAs, 0.8 pitch, and standard filters.

SPECT emission data were processed by using the filtered backprojection method with CT-based attenuation correction. A Butterworth filter with cutoff frequency of 0.2/cm was applied. Twenty-seven SPECT volumes (matrix: 128 × 128 × 142; resolution: 3.9 × 3.9 × 2.5 mm^3) were reconstructed, in which the volumes 1–8, 9–14, 15–19, 20–21, 22–24, and 25–27 were with time intervals of 15 s, 30 s, 1 min, 2.5 min, 5 min, and 10 min, respectively. The time–activity curve of each voxel was obtained by interpolating the 27 sampling points to have a time interval of 15 s (Fig. 1).

2.B. ICG clearance test

The validity of HEF determination was evaluated by comparing to ICG clearance time (T1/2). ICG testing was performed at ±1 day of each SPECT/CT scan. Two intravenous catheters, one for ICG infusion and the other for drawing blood samples, were used. Immediately after bolus administration of ICG dye (0.5 mg/kg), blood samples (~6 ml) were drawn at time of 0, 5, 10, 15, and 20 min. The half-life time (T1/2) of ICG clearance was determined by evaluating the ICG concentration decay in the serum samples.[17]

2.C. Deconvolution analysis

Mathematically, a liver time–activity curve [$l(t)$] is yielded from a convolution between a blood input function [$b(t)$] and an impulse response function [$h(t)$] (Fig. 2):[3]

$$l(t) = b(t) \otimes h(t), \tag{1}$$

where $t = n\Delta t$ ($n = 0, 1, \ldots, N-1$) is time sampling a function with a time interval of Δt. With the knowledge of the blood input and the liver time–activity curve, the impulse response function can be estimated by deconvolution computation.

We formulated the convolution into matrix form $L = B \cdot H$, where

$$L = \begin{bmatrix} l(0) \\ l(1) \\ \vdots \\ l(N-1) \end{bmatrix}, \quad B = \begin{bmatrix} b(0) & 0 & \ldots & 0 \\ b(1) & b(0) & \ldots & 0 \\ \vdots & \vdots & \vdots & \vdots \\ b(N-1) & b(N-2) & \ldots & b(0) \end{bmatrix}, \quad H = \begin{bmatrix} h(0) \\ h(1) \\ \vdots \\ h(N-1) \end{bmatrix}. \tag{2}$$

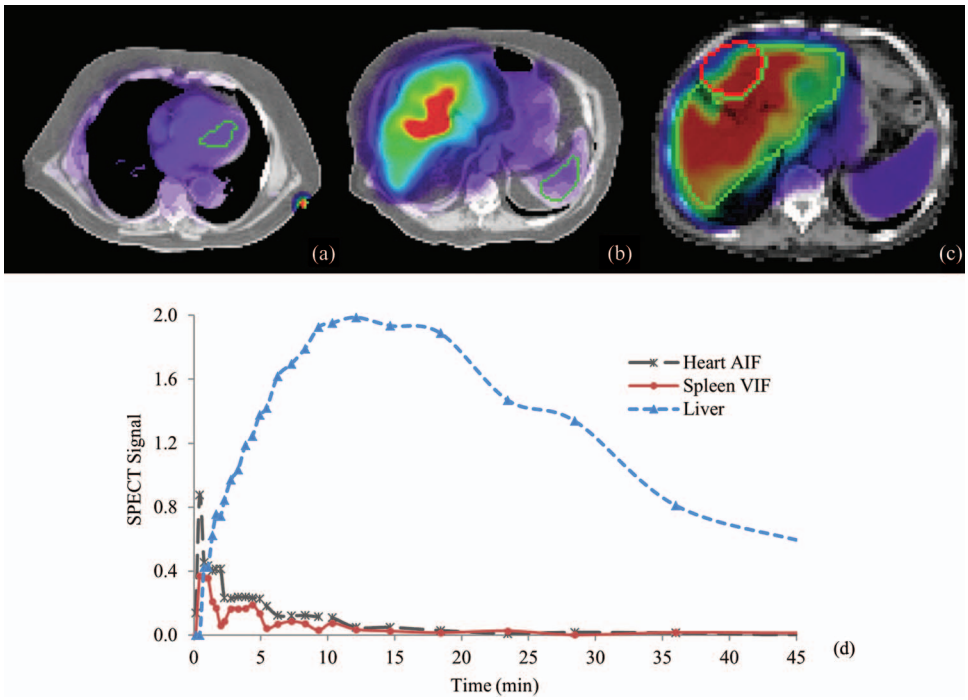

FIG. 1. Color mapped SPECT overlapped on CT with ROIs drawn on the heart for an AIF (a) and on the spleen for a VIF (b). (c) Nontumor liver tissue contoured on the liver and a tumor contoured by the circle. (d) Plots dynamic SPECT curves of a liver voxel, AIF from the heart and VIF from the spleen (b).

In order to solve the equation for H, square matrix B is decomposed by singular value decomposition (SVD)

$$B = U \cdot W \cdot V^T, \tag{3}$$

where U and V are orthogonal, and W is diagonal with the elements $w_0 \geq w_1 \geq w_2 \geq \cdots \geq w_{N-1} \geq 0$. Then H is solved as

$$H = V \cdot \left[\text{diag}\left(\frac{1}{w_i}\right)\right] \cdot U^T \cdot L. \tag{4}$$

Noise in the data will be magnified due to the inversion of W if one or more w_i values are zero or close to zero. The truncated SVD method was used to resolve this problem, in which a threshold c was defined and $1/w_i$ was calculated only for $w_i \geq c$. We heuristically determined c to ensure the HEFs in normal liver tissue regions close to 100%. In this study, we used 1% of the maximal singular value (w_0) as c and 15 s for the time interval Δt.

2.D. Hepatic extraction fraction estimation

The impulse response function [$h(t)$] resulting from the SVD-based deconvolution describes the response of liver parenchyma to a single bolus of IDA agent injected directly into the hepatic vasculature without subsequent recirculation. Because of the time delay for blood input bolus reaching the liver parenchyma, the impulse response function began with a sharp increase and then divided into the vascular phase and the hepatocyte retention phase (Fig. 2).[3] Following the conventional approach,[3,10] we fitted the retention phase in $h(t)$ with an exponential function, and then extrapolated the exponential function back to the initial time of the hepatocyte retention when the activity of the vascular phase was maximal. Finally, HEF was computed as the ratio between the fitted activity at the initial time of the hepatocyte retention and the peak activity of the vascular phase:

$$\text{HEF} = \frac{\text{fitted initial hepatocyte retention}}{\text{peak of vascular phase}}. \tag{5}$$

Least squares minimization was performed for the exponential fitting of the retention phase in the impulse response

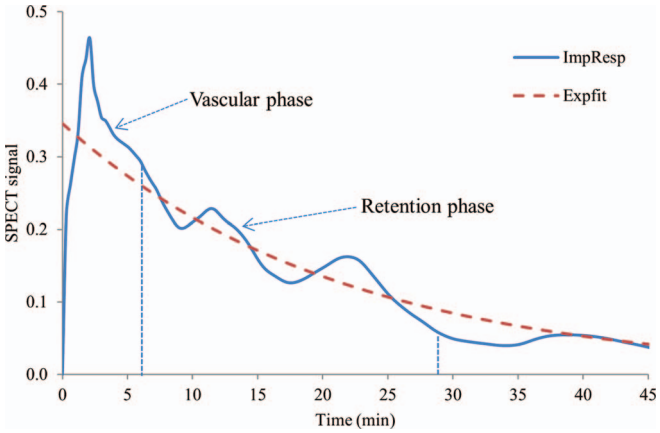

FIG. 2. Impulse response function from deconvolution for HEF estimation. The deconvolution was done between a SPECT curve of a liver voxel and the VIF from the spleen. Time course of 7–30 min was defined as the retention phase of the impulse response function. Exponential fitting of the retention phase is shown and extrapolated to initial time of the retention when the vascular phase was maximal.

function. The time range for the retention phase needs to be specified before the fitting. It is generally accepted that the secretion of IDA becomes dominant approximately 30 min after injection,[10] and a number of studies defined the retention phase between 6 and 30 min after the injection of IDA agent.[3,10] For the patients with intrahepatic cancers, we examined time ranges of 6–30 min (T6-30), 7–30 min (T7-30), and 8–30 min (T8-30) for the retention phase to determine the impact of the time range parameter on voxelwise HEF quantification.

Normal liver parenchyma extracts 95%–100% of 99mTc-mebrofenin in incoming blood, and thus the HEF is close to 1.[10] Hepatocytes in damaged liver tissue are only able to retain a small portion of the total IDA agent, indicating a HEF less than 1. Therefore, the HEF is supposed to be bounded between 0 and 1. However, due to image noise and artifacts, the voxelwise HEF may be beyond the range, particularly, at the voxels in normal liver parenchyma. In this study, we also calculated the percentage of voxels whose HEFs were within the range in order to evaluate the reliability of the HEF estimation.

2.E. Input function determination and image analysis

The blood input function $b(t)$ in the deconvolution analysis was obtained from a ROI on the heart in most 99mTc-IDA scintigraphy studies of hepatocellular function.[3,4,6,9,11] In this SPECT/CT study, we compared the voxelwise HEF estimation using AIF from the heart with the estimation using VIF from the spleen. On the axial CT of the SPECT/CT, ROIs were delineated on the left ventricle of the heart and the spleen. In order to minimize spillover and partial-volume effects in SPECT, the ROI on the heart was placed at least 2 pixels away from the heart wall, and the ROI on the spleen was also at least 2 pixels away from the boundary of the spleen. We selected the SPECT volume that had peak activity on the time–activity curve for the heart ROIs, and then iteratively used a stepwise threshold to remove low SPECT activity until the ROI had approximate 100 voxels. Similarly, we generated a ROI with 100–200 voxels on the spleen. The AIF and the VIF were the time–activity curves of mean activity on respective ROI. Figure 1 shows the ROIs on the heart [Fig. 1(a)] and the spleen [Fig. 1(b)] from which the AIF and the VIF were generated [Fig. 1(c)].

The liver was delineated on the CT of the SPECT/CT. To mitigate partial volume effect on the HEF estimation, 2 pixels from the delineated boundary of the liver were excluded by morphological erosion on each image plane. Care was also taken to exclude major blood vessels, visible bile ducts, and gallbladder from the liver. The HEFs of the liver before and one month after RT were estimated voxel-by-voxel using the AIF and the VIF, as well as the three time ranges for the retention phase (T6-30, T7-30, and T8-30). To evaluate the reliability of the voxelwise HEF estimation, a ROI was drawn on the nontumor liver region with relatively homogenous tissue. The ROI was placed far away from tumors and with the planned radiation dose less than 10 Gy that seems to have minimal effect in the liver.[18]

2.F. Statistical analysis

Descriptive statistics [mean, standard deviation (std), median, maximum, and minimum] was calculated for the HEFs in each ROI with respect to the use of the AIF or the VIF and the time ranges for the retention phase. The means of the HEFs in the ROIs were compared between using the AIF and the VIF by paired t-test. The test was also performed between the time ranges for the retention phase. To evaluate the uncertainty of the voxelwise HEF estimation, we calculated the relative variation of the HEFs in the ROIs, which was calculated as the ratio of standard deviation to the mean of the HEFs.

Mean of the HEFs over a whole liver excluding gross tumor volumes [Fig. 1(c)] was calculated. Any HEF above 1 was set as 1 in the mean HEF calculation. We evaluated the correlation between mean of the HEFs over the liver and the ICG clearance half-time T1/2 by Spearman's rank correlation coefficient (r) on all imaging sessions. ICG clearance test is clinically used to measure overall liver function, therefore the correlation between the mean of the HEFs over the liver and the T1/2 verified the voxelwise HEFs as measure of liver function. The statistical package of R was used,[19] and a two-sided p-value less than 0.05 was considered statistically significant.

3. RESULTS

Means of the HEFs in the drawn ROIs for all imaging sessions were compared with respect to the AIF from the heart and the VIF from the spleen (Fig. 3). The ROIs have a size of 1845 ± 659 voxels. As the ROIs were drawn away from the tumors, the median HEF is around 0.8 when computing with the AIF and is around 0.7 if using the VIF, regardless of the given time ranges for the retention phase. The t-test (Table I) shows significant difference in the mean HEFs of the ROIs between using the AIF and the VIF ($p < 0.0001$). However, using either the AIF or the VIF, there is no significant difference in the mean ROI HEFs between the three time ranges

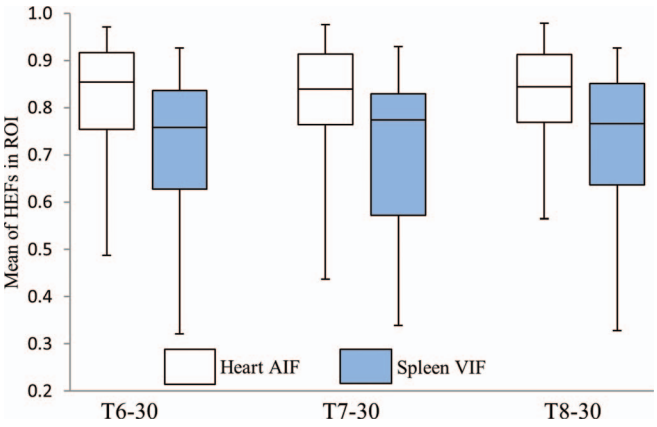

FIG. 3. Distribution of means of HEFs in the ROIs of the patients estimated with AIF from the heart and VIF from the spleen. The ROIs (~1845 voxels) were drawn on the liver tissue far away from the tumor and receiving radiation dose less than 10 Gy.

TABLE I. Paired *t*-test for means of HEFs in the ROIs.

	T6-30		T7-30		T8-30	
	AIF	VIF	AIF	VIF	AIF	VIF
Mean	0.83	0.71	0.83	0.71	0.82	0.70
Standard deviation	0.12	0.16	0.11	0.16	0.13	0.18
t-test between using AIF and VIF (*p*-value)	1.09×10^{-6}		3.55×10^{-6}		1.38×10^{-5}	
	T6-30	T7-30	T7-30	T8-30	T6-30	T8-30
t-test between time ranges with using AIF (*p*-value)	0.06		0.47		0.52	
t-test between time ranges with using VIF (*p*-value)	0.39		0.1		0.23	

for the retention phase ($p > 0.05$), suggesting that the HEF estimation is relatively robust to the selection of time range for the retention phase.

The correlation for a total of 28 pairs of means of liver HEFs and ICG clearance T1/2 is shown in Fig. 4. The HEFs were estimated with the time range of 7–30 min for the retention phase. Although the means of the live HEFs estimated with the AIF and the VIF both are significantly correlated with the T1/2 ($p = 0.0004$ for the AIF, and $p < 0.0001$ for the VIF), the correlation of the mean of HEFs estimated with the VIF is much better ($r = 0.79$) than using the AIF ($r = 0.52$). The correlations indicate that the voxelwise HEF derived from 99mTc-mebrofenin SPECT using VIF is able to assess hepatic function. Using the VIF and the retention phase time ranges of 6–30 and 8–30 min, the Spearman's correlation coefficients between the mean of the HEFs over the liver and the T1/2 are 0.78 and 0.76, respectively, indicating the robustness of the HEF estimation to the time range parameter. Based on the correlation coefficients, VIF and the retention phase time range 7–30 min could be used to estimate the HEF voxel-by-voxel from 99mTc-mebrofenin SPECT for evaluating spatially resolved hepatic function.

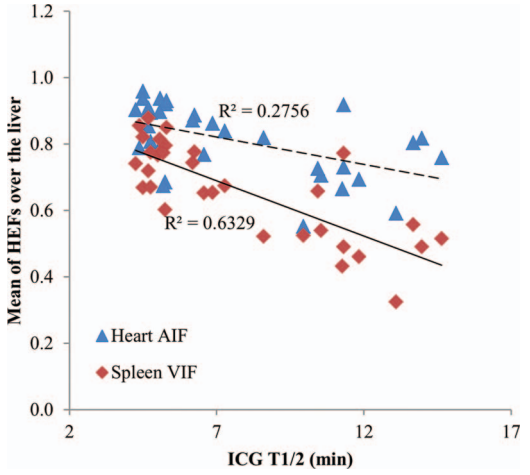

FIG. 4. Correlation between ICG T1/2 and mean of HEFs over the nontumor liver tissue estimated using the AIF in the heart and the VIF from the spleen. The retention phase was set as 7–30 min.

We next evaluated the variation of the HEF estimated with the VIF. Figure 5 compares the relative variations of the voxelwise HEF in the drawn ROIs among the three time range settings. In the ROIs, there are no significant differences in the HEF relative variations for any paired time ranges of the retention phase ($p > 0.4$). The range of the relative variation of the HEFs in the ROIs estimated with T7-30 (mean: 10%; std: 6%) is 5%–25% that is smaller than the ranges of 5%–54% and 4%–33% for the HEFs estimated with T6-30 and T8-30, respectively. Considering the relative variation of SPECT intensities in these ROIs with a mean value of 15% (std: 6%), the variation of the HEF estimated with a VIF and T7-30 indicates the feasibility of the HIDA SPECT-derived HEF for spatial quantification of liver function. The percentage of voxels with a HEF not greater than 1 was calculated for each imaging session. In all the tumor-excluded livers (volume: 1092 $\pm$ 460 cm^3), 89% $\pm$ 7% of the volume has voxelwise HEFs not greater than 1, suggesting the reliability of the HEF quantification to some extent.

Parametric maps of the HEF in the liver before and one month after RT for one patient are shown in Fig. 6. The HEF was estimated with VIF and the retention phase of 7–30 min after the injection of 99mTc-mebrofenin. Radiation therapy led to reduction of the HEF one month after the treatment, and the amplitude of reduction seems greater at the region close to the planning target volume (marked circles) where the highest radiation dose was delivered to treat the cholangiocarcinoma.

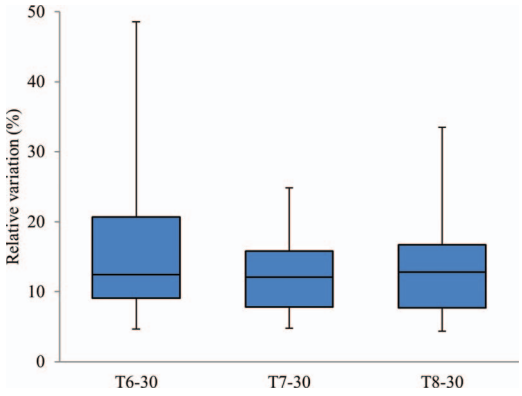

FIG. 5. Relative variations of HEFs in the ROIs estimated using the VIF and different time ranges for the retention phase.

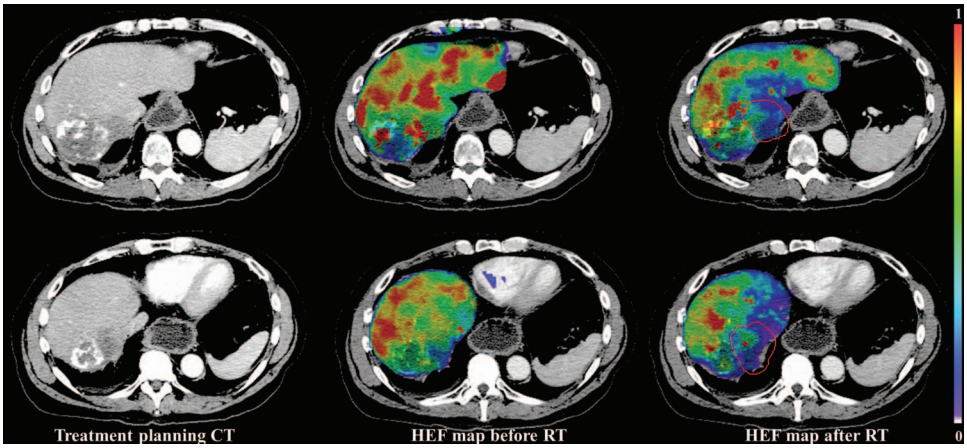

FIG. 6. HEF maps overlapped on treatment planning CT. Left are slices of the treatment planning CT, middle and the right are color mapped HEFs before and 1 month after RT, respectively, overlapped on the CT. The HEF was estimated voxel-by-voxel using the VIF and 7–30 min for the retention phase. Any HEF above 1 is displayed as 1. Planning target regions (PTV) that received highest radiation dose are shown as the circles on the right figures.

4. DISCUSSION

In this study, the performance of the voxelwise HEF estimation was evaluated with respect to the blood input functions from the heart and the spleen, as well as the parameter of time range for the retention phase. The mean of the HEFs over the liver estimated with the VIF from the spleen shows a much more significant correlation with the overall liver function compared with the mean of HEFs estimated with the AIF from the heart. In contrast to the 99mTc-IDA scintigraphic studies of hepatic function in whole organ or ROI level, the study demonstrates the feasibility of 99mTc-IDA SPECT to spatially assess hepatic function of the patients with intrahepatic cancers.

Our study estimated the HEF voxel-by-voxel from 99mTc-mebrofenin SPECT acquired on a hybrid SPECT/CT scanner to assess hepatic function with spatial distribution. The HEF was evaluated in the ROIs that were placed to have hepatic function as homogeneous as possible. Our results show the estimation is rather insensitive to the parameter of time range for the retention phase regardless using the AIF from the heart or the VIF from the spleen. Furthermore, we show that the volumetric-weighted mean HEF of the liver significantly correlates with the global liver function measured by the ICG clearance test, and the correlation using the VIF is much better than the correlation using the AIF. The correlation is robust for the patients with primary or metastatic liver cancers and having a wide range of liver functions (T1/2: 4.25–14.64 min). Currently, liver function is most often assessed by serum analyte measurements or scoring based on clearance tests.[14] These tests can assess the overall liver function, but cannot investigate hepatic function in a regional or segmental manner. Therefore, the volumetric HEF derived from 99mTc-IDA SPECT provides complementary spatial information for the global hepatic function.

The knowledge of IDA blood input function is required for HEF estimation. Previously, the input function was usually obtained from a ROI on the heart as the planar scintigraphy did not have detailed anatomical information. In this study, with an anatomical CT of SPECT/CT, we have shown that the VIF from the spleen achieved better correlation between the mean of HEFs over the liver and the overall liver function measured by the ICG clearance test. The results suggest that the bolus passage of IDA agents in the spleen vessels may be more representative of the bolus in the capillaries of the liver. The liver has dual blood inputs from the portal vein and the hepatic artery. While the majority of blood supply to liver tumor is from the hepatic artery, normal liver tissue derives approximately 85% of its blood supply from the portal vein.[20] Therefore, for nontumor liver tissue evaluated for hepatic function, the VIF from a ROI on the spleen that is composed of both artery and vein voxels may better indicate the dynamic of the tracer input to the liver than the AIF from the heart. To assess hepatic extraction using hepatocyte-specific contrast-enhanced MRI in healthy volunteers, the VIF directly obtained from the pixels in the portal vein was used by others.[21] Due to the difficulty of identifying the portal vein in SPECT/CT, we believe that the input function from the spleen is a valid choice for the HEF quantification from 99mTc-IDA SPECT, particularly, to assess treatment-induced liver damage in which the hepatic function in the nontumor liver tissue is mostly considered. This study estimated HEF from dynamic SPECT images without scatter correction. For 99mTc SPECT images, the ratio of scattered to primary photons in the photopeak energy window could be as high as about 30%. However, The HEF is calculated as a ratio derived from the impulse response function, which only depends on the shape of the dynamic curve at a voxel. Therefore, scatter may have less effect on the voxelwise HEF quantification.

Increasing radiation dose for better radiation therapy of liver cancer is limited by the development of radiation-induced liver disease.[22] Likewise, the major cause for postoperative mortality after liver surgery is the liver failure.[23] This study shows the potential of 99mTc-IDA SPECT to depict hepatic function in a voxel or regional level. The spatially resolved imaging of liver function could be used to investigate treatment toxicity in the liver and certainly be of great

value in treatment planning for radiation therapy or resection of liver cancer, by which the normally functioning liver regions can be preserved to minimize liver injury while poorly functioning liver segments can be sacrificed for optimal tumor ablation. Furthermore, assessing liver function response to therapy by 99mTc-IDA SPECT may enable prediction of treatment-induced liver complication, and thereby reoptimize treatment planning for liver cancer during the therapy. Further studies are required to assess the reproducibility of the voxelwise HEF quantification, and to evaluate the relationship between the regional HEF change and the applied treatment. In this examination of 99mTc-mebrofenin SPECT for assessment of hepatic function response to therapy, we focused on evaluating the HEF in the nontumor liver voxels. The potential of HEF quantification and 99mTc-IDA SPECT to assess residual hepatic function in liver cancer may be investigated in the future.

5. CONCLUSIONS

Spatially resolved hepatic function in the liver can be evaluated by using the voxelwise HEF derived from 99mTc-IDA SPECT. By the deconvolution analysis with a vascular input function from the spleen, the mean HEF of the liver correlated with the overall liver function assessed by an independent physiological measurement. 99mTc-IDA SPECT and the voxelwise HEF may provide a tool to assess liver function response to therapy to minimize treatment-induced liver dysfunction.

ACKNOWLEDGMENT

This work was supported in part by RO1 CA132834.

[a]Author to whom correspondence should be addressed. Electronic mail: hesheng@umich.edu

[1]T. Aburano, K. Yokoyama, N. Shuke, T. Takayama, T. Michigishi, N. Tonami, K. Hisada, M. Unoura, and K. Kobayashi, "99mTc colloid and 99mTc IDA imagings in diffuse hepatic disease," J. Clin. Gastroenterol. **17**, 321–326 (1993).

[2]T. Aburano, K. Yokoyama, N. Shuke, S. Kinuya, T. Takayama, N. Tonami, and K. Hisada, "The role of Tc-99m IDA hepatobiliary and Tc-99m colloid hepatic imaging in primary biliary cirrhosis," Clin. Nucl. Med. **16**, 4–9 (1991).

[3]J. E. Juni and R. Reichle, "Measurement of hepatocellular function with deconvolutional analysis: Application in the differential diagnosis of acute jaundice," Radiology **177**, 171–175 (1990).

[4]E. Jonas, E. Naslund, J. Freedman, R. Befrits, L. Blomqvist, A. K. Siosteen, H. Jacobsson, and R. Hultcrantz, "Measurement of parenchymal function and bile duct flow in primary sclerosing cholangitis using dynamic 99mTc-HIDA SPECT," J. Gastroenterol. Hepatol. **21**, 674–681 (2006).

[5]M. Michael, M. Thompson, R. J. Hicks, P. L. Mitchell, A. Ellis, A. D. Milner, J. Di Iulio, A. M. Scott, V. Gurtler, J. M. Hoskins, S. J. Clarke, N. C. Tebbut, K. Foo, M. Jefford, and J. R. Zalcberg, "Relationship of hepatic functional imaging to irinotecan pharmacokinetics and genetic parameters of drug elimination," J. Clin. Oncol. **24**, 4228–4235 (2006).

[6]I. Roca and G. Ciofetta, "Hepatobiliary scintigraphy in current pediatric practice," Q. J. Nucl. Med. **42**, 113–118 (1998).

[7]H. Wang, M. Feng, K. A. Frey, R. K. Ten Haken, T. S. Lawrence, and Y. Cao, "Predictive models for regional hepatic function based on 99mTc-IDA SPECT and local radiation dose for physiologic adaptive radiation therapy," Int. J. Radiat. Oncol., Biol., Phys. **86**, 1000–1006 (2013).

[8]G. T. Krishnamurthy and F. E. Turner, "Pharmacokinetics and clinical application of technetium 99m-labeled hepatobiliary agents," Semin. Nucl. Med. **20**, 130–149 (1990).

[9]P. H. Brown, J. E. Juni, D. A. Lieberman, and G. T. Krishnamurthy, "Hepatocyte versus biliary disease: A distinction by deconvolutional analysis of technetium-99m IDA time-activity curves," J. Nucl. Med. **29**, 623–630 (1988).

[10]E. Doo, G. T. Krishnamurthy, M. J. Eklem, S. Gilbert, and P. H. Brown, "Quantification of hepatobiliary function as an integral part of imaging with technetium-99m-mebrofenin in health and disease," J. Nucl. Med. **32**, 48–57 (1991).

[11]R. Howman-Giles, A. Moase, K. Gaskin, and R. Uren, "Hepatobiliary scintigraphy in a pediatric population: Determination of hepatic extraction fraction by deconvolution analysis," J. Nucl. Med. **34**, 214–221 (1993).

[12]M. T. Madsen, "Recent advances in SPECT imaging," J. Nucl. Med. **48**, 661–673 (2007).

[13]Z. Keidar, O. Israel, and Y. Krausz, "SPECT/CT in tumor imaging: Technical aspects and clinical applications," Semin. Nucl. Med. **33**, 205–218 (2003).

[14]S. G. Sakka, "Assessing liver function," Curr. Opin. Crit. Care **13**, 207–214 (2007).

[15]A. W. Hemming, C. H. Scudamore, C. R. Shackleton, M. Pudek, and S. R. Erb, "Indocyanine green clearance as a predictor of successful hepatic resection in cirrhotic patients," Am. J. Surg. **163**, 515–518 (1992).

[16]M. E. Gottlieb, H. H. Stratton, J. C. Newell, and D. M. Shah, "Indocyanine green. Its use as an early indicator of hepatic dysfunction following injury in man," Arch. Surg. **119**, 264–268 (1984).

[17]G. R. Cherrick, S. W. Stein, C. M. Leevy, and C. S. Davidson, "Indocyanine green: Observations on its physical properties, plasma decay, and hepatic extraction," J. Clin. Invest. **39**, 592–600 (1960).

[18]L. A. Dawson, D. Normolle, J. M. Balter, C. J. McGinn, T. S. Lawrence, and R. K. Ten Haken, "Analysis of radiation-induced liver disease using the Lyman NTCP model," Int. J. Radiat. Oncol., Biol., Phys. **53**, 810–821 (2002).

[19]R Development Core Team, *R: A Language and Environment for Statistical Computing* (R Foundation for Statistical Computing, Vienna, Austria, 2012).

[20]P. V. Pandharipande, G. A. Krinsky, H. Rusinek, and V. S. Lee, "Perfusion imaging of the liver: Current challenges and future goals," Radiology **234**, 661–673 (2005).

[21]H. Nilsson, A. Nordell, R. Vargas, L. Douglas, E. Jonas, and L. Blomqvist, "Assessment of hepatic extraction fraction and input relative blood flow using dynamic hepatocyte-specific contrast-enhanced MRI," J. Magn. Reson. Imaging **29**, 1323–1331 (2009).

[22]B. Emami, J. Lyman, A. Brown, L. Coia, M. Goitein, J. E. Munzenrider, B. Shank, L. J. Solin, and M. Wesson, "Tolerance of normal tissue to therapeutic irradiation," Int. J. Radiat. Oncol., Biol., Phys. **21**, 109–122 (1991).

[23]J. T. Mullen, D. Ribero, S. K. Reddy, M. Donadon, D. Zorzi, S. Gautam, E. K. Abdalla, S. A. Curley, L. Capussotti, B. M. Clary, and J. N. Vauthey, "Hepatic insufficiency and mortality in 1,059 noncirrhotic patients undergoing major hepatectomy," J. Am. Coll. Surg. **204**, 854–862 (2007).